**Supplemental Proceedings: Volume 2: Materials Properties, Characterization, and Modeling**
***TMS (The Minerals, Metals & Materials Society), 2012***

# FINITE ELEMENT IMPLEMENTATION OF A SELF-CONSISTENT POLYCRYSTAL PLASTICITY MODEL: APPLICATION TO α-URANIUM

Marko Knezevic, Rodney J. McCabe, Ricardo A. Lebensohn,
Carlos N. Tomé, and Bogdan Mihaila

Materials Science and Technology Division, Los Alamos National Laboratory,
Los Alamos, NM 87545, USA

Keywords: Uranium, Constitutive Modeling, Finite Element Method

## Abstract

We present an improved implementation of the viscoplastic self-consistent (VPSC) polycrystalline model in an implicit finite element (FE) framework, which accounts for a dislocation-based hardening law for multiple slip and twinning modes at the micro-scale crystal level. The model is applied to simulate at the macro-scale the highly anisotropic mechanical response of wrought α-uranium. In doing this, a finite element integration point is considered as a polycrystalline material point, whose meso-scale mechanical response is obtained by the mean-field VPSC homogenization scheme. Simple compression, simple tension, and simple shear tests on polycrystalline wrought uranium are used to demonstrate the accuracy of the implemented model.

## Introduction

Polycrystal plasticity models have been extensively used to understand and predict the mechanical response and microstructure evolution (mostly texture-related aspects) in metals subject to finite strains, e.g [1-4]. The degree of sophistication necessary to model accurately a material generally correlates with the number and types of deformation modes active in a material. Uranium, an important metal for nuclear fuels and defense applications, is a challenging material to model because it exhibits 4 different slip modes and 3 different deformation twinning modes. Moreover, the operating slip and twinning modes exhibit low multiplicity and widely different activation stresses. Consequently, the plastic response is markedly anisotropic and hardening depends strongly on texture and on the interactions between the slip and twin modes. We have recently showed that a hardening law explicitly based on dislocation density evolution implemented within the VPSC homogenization scheme performs well in capturing the anisotropic strain-hardening and the texture evolution in uranium [5]. In turn, this provides an incentive for incorporating a VPSC-based material subroutine for uranium into a finite element framework to facilitate process design and mechanical evaluation of uranium components.

The strategy of embedding the mean-field VPSC model at the meso-scale level in an implicit FE analysis was discussed in [6]. In an implicit nonlinear FE formulation, the material constitutive model provides the stress and tangent stiffness matrix. In the recent development, the tangent stiffness matrix (Jacobian) is obtained analytically and allows for fast convergence towards stress equilibrium. This FE Jacobian is obtained as a function of the viscoplastic tangent moduli (which has already been calculated as part of the nonlinear self-consistent homogenization scheme), the elastic stiffness of the aggregate, and the FE time increment.

In this paper, we combine these recent advances and present an implementation of the VPSC polycrystalline model in implicit finite elements that accounts for a dislocation-density-based

hardening law necessary to model the highly anisotropic response of α-uranium. In addition, we demonstrate that the VPSC calculations can be performed in the global FE frame rather than in the co-rotational frame adopted in the original implementation [6]. Simple compression, simple tension, and simple shear tests on polycrystalline wrought uranium are used to demonstrate the accuracy of the implemented model.

## Micro-Scale Model

The equations underlying the single crystal dislocation-density-based hardening law implemented within VPSC were discussed in [7, 8] and are briefly summarized here. Plastic deformation in each grain occurs via the activation of both slip and twin modes. The corresponding slip or twin shear rate, $\dot{\gamma}^s$, on a given system, *s*, is given by the power-law:

$$\dot{\gamma}^s = \dot{\gamma}_o \left| \frac{\tau^s}{\tau_c^s} \right|^{\frac{1}{m}} sign\left(\tau^s\right) \tag{1}$$

Here, $\dot{\gamma}_o^s$, *m*, $\tau^s$, and $\tau_o^s$, are the reference slip rate, the rate-sensitivity exponent, resolved shear stress and critical resolved shear stress (CRSS) on the slip/twin system, respectively.

Consistent with experimental evidence, the following four slip modes (010)[100], (001)[100], ½{110}<1-10> and ½{1-12}<021> and two twin modes {130}<3-10> and {172}<3-12> are considered as potential systems for accommodating the imposed plastic strain. A rate-sensitivity exponent, m=0.1, is taken to be the same for all slip and twinning modes. The critical resolved shear stresses (CRSS) of all slip systems or twin variants within one mode α (or family) in a grain are assumed to exhibit the same resistance. In the case of slip, the CRSS is expressed as a sum of a friction stress $\tau_o^\alpha$, a forest dislocation interaction stress $\tau_{for}^\alpha$, and a dislocation substructure interaction stress $\tau_{sub}^\alpha$, i.e.

$$\tau_c^s = \tau_o^\alpha + \tau_{for}^\alpha + \tau_{sub}^\alpha \tag{2}$$

The evolution of $\tau_{for}^\alpha$ and $\tau_{sub}^\alpha$ is governed by the evolution of the forest $\rho_{for}^\alpha$ and substructure $\rho_{sub}^\alpha$ dislocation densities, as explained in detail in [8]. The CRSS for twin activation accounts for the friction term $\tau_c^\beta$ and a latent hardening term coupling slip and twin systems. The critical resolved shear stress for twinning is given by

$$\tau_c^\beta = \tau_o^\beta + \mu^\beta \sum_\beta C^{\alpha\beta} b^\beta b^\alpha \rho_{for}^\alpha \tag{3}$$

Here, $\mu^\beta$, $b^\beta$ and $C^{\alpha\beta}$ are the elastic shear modulus on the system, the Burgers vector or shear direction of a given system, and the latent hardening matrix, respectively. The twin transformation is modeled via the composite grain (CG) model [9]. In brief, CG consists of identifying in each grain the twin system with the highest shear rate among all active twin systems, i.e. the predominant twin system (PTS), and partitioning the grain into a stack of flat ellipsoids having the crystallographic orientation of the predominant twin and the matrix, respectively. The short axes of the ellipsoids are perpendicular to the twin plane. As shear is

being accommodated by the twin, the corresponding volume fraction is transferred from the parent to the twin. The ellipsoids representing the twins thicken and the ones representing the parent shrink. Except for the volume transfer coupling, the twin and the parent ellipsoids are treated as independent inclusions in the model.

**Meso-Scale Model**

At polycrystal level, the use of a rigid-viscoplastic approach implies that the constitutive relations at single-crystal level can be expressed in terms of Cauchy stress deviator $\boldsymbol{\sigma}'$ and the (Eulerian) viscoplastic strain-rate $\dot{\boldsymbol{\varepsilon}}_{\mathrm{vp}}$[1]:

$$\dot{\varepsilon}_{vp}(\mathbf{x}) = \sum_{k=1}^{N_k} m^k(\mathbf{x})\dot{\gamma}^k(\mathbf{x}) \tag{4}$$

where the sum runs over all $N_k$ slip and twin systems and $m^k$ is the Schmid tensor associated with slip or twinning system $k$. A linear relation (an approximation of the actual local nonlinear relation, Eq. 3) is assumed between $\dot{\boldsymbol{\varepsilon}}_{\mathrm{vp}}^{(\mathrm{r})}$ and $\boldsymbol{\sigma}'^{(\mathrm{r})}$, i.e.

$$\dot{\boldsymbol{\varepsilon}}_{\mathrm{vp}}^{(\mathrm{r})} = \boldsymbol{M}^{(\mathrm{r})} : \boldsymbol{\sigma}'^{(\mathrm{r})} + \dot{\boldsymbol{\varepsilon}}^{\mathrm{o}(\mathrm{r})} \tag{5}$$

where $\boldsymbol{M}^{(\mathrm{r})}$ and $\dot{\boldsymbol{\varepsilon}}^{\mathrm{o}(\mathrm{r})}$ are the linearized viscoplastic compliance and back-extrapolated strain-rate of grain (r), respectively. The behavior of the single crystals can be homogenized assuming a linear relation at the effective medium (polycrystal, *px*) level:

$$\dot{\boldsymbol{\varepsilon}}_{\mathrm{vp}}^{(\mathrm{px})} = \boldsymbol{M}^{(\mathrm{px})} : \boldsymbol{\sigma}'^{(\mathrm{px})} + \dot{\boldsymbol{\varepsilon}}^{\mathrm{o}(\mathrm{px})} \tag{6}$$

where $\dot{\boldsymbol{\varepsilon}}_{\mathrm{vp}}^{(\mathrm{px})}$ and $\boldsymbol{\sigma}'^{(\mathrm{px})}$ are the effective (polycrystal) deviatoric strain-rate and stress tensors and $\boldsymbol{M}^{(\mathrm{px})}$ and $\dot{\boldsymbol{\varepsilon}}^{\mathrm{o}(\mathrm{px})}$ are the tangent viscoplastic compliance and back-extrapolated strain-rate of an a priori unknown homogeneous medium that represents the behavior of the polycrystal. The usual procedure to obtain the homogenized response of a linear polycrystal is the linear self-consistent method. The problem underlying the self-consistent method is that of a single crystal *r* of moduli $\boldsymbol{M}^{(\mathrm{r})}$ and $\dot{\boldsymbol{\varepsilon}}^{\mathrm{o}(\mathrm{r})}$, embedded in an infinite medium of moduli $\boldsymbol{M}^{(\mathrm{px})}$ and $\dot{\boldsymbol{\varepsilon}}^{\mathrm{o}(\mathrm{px})}$, which can be obtained using standard self-consistent analysis.

The above numerical scheme can be used to predict the stress-strain response and the microstructure evolution of the polycrystal (crystallographic and morphologic texture and hardening evolution), by applying the viscoplastic deformation to the polycrystal in incremental steps. The latter is performed assuming constant rates during a time interval $\Delta\mathrm{t}$ and using the strain-rates $\dot{\boldsymbol{\varepsilon}}_{\mathrm{vp}}^{(\mathrm{r})}$ and rotation-rates $\dot{\boldsymbol{\omega}}^{(\mathrm{r})}$ (times $\Delta\mathrm{t}$) to update the shape and orientation of the grains. The shear rates (times $\Delta\mathrm{t}$) are used to update the critical stress of the deformation systems due to strain hardening, after each deformation increment.

**Macro-Scale Model**

In our implementation of VPSC as an UMAT in ABAQUS-Standard, we write the total strain increment ( $\Delta\boldsymbol{\varepsilon}$ ) as the sum of the elastic ( $\Delta\boldsymbol{\varepsilon}_{\mathrm{el}}$ ) and viscoplastic ( $\Delta\boldsymbol{\varepsilon}_{\mathrm{vp}}$ ):

$$\Delta\boldsymbol{\varepsilon} = \Delta\boldsymbol{\varepsilon}_{\mathrm{el}} + \Delta\boldsymbol{\varepsilon}_{\mathrm{vp}} = \boldsymbol{C}^{-1} : \Delta\boldsymbol{\sigma} + \Delta\boldsymbol{\varepsilon}_{\mathrm{vp}} \tag{7}$$

where $\boldsymbol{C}$ is the elastic stiffness of the polycrystalline material point, $\Delta\boldsymbol{\sigma}$ is the Cauchy stress increment, and $\Delta\boldsymbol{\varepsilon}_{\mathrm{vp}} = \Delta\boldsymbol{\varepsilon}_{\mathrm{vp}}(\boldsymbol{\sigma})$ is computed using the VPSC model for each polycrystalline material point.

In an earlier work [6], the VPSC calculations were performed in a local co-rotational and the texture was represented in this moving frame. In our new implementation, the polycrystalline material undergoes the macroscopically-imposed rotation at every time increment, in addition to a rotation due to the plastic spin and antisymmetric part of the Eshelby tensor. The polycrystal elastic stiffness and the viscoplastic strain increment are calculated using the VPSC model in the global frame. The benefit of the new implementation is that field variables are *not* rotated between the global and co-rotational frame.

The macro-scale constitutive model is formulated incrementally, using the Jaumann rate:

$$\overset{\nabla}{\boldsymbol{\sigma}} = \boldsymbol{C} : \left(\dot{\boldsymbol{\varepsilon}} - \dot{\boldsymbol{\varepsilon}}_{\mathrm{vp}}\right) \tag{8}$$

Integrating Eq. (8) from time $t$ to $t + \Delta t$ gives:

$$\overset{\nabla}{\boldsymbol{\sigma}}\,\Delta \mathrm{t} = \boldsymbol{C} : \left(\Delta\boldsymbol{\varepsilon} - \Delta\boldsymbol{\varepsilon}_{\mathrm{vp}}\right) \tag{9}$$

At macroscopic level, the applied load is divided in increments, and the equilibrium at each increment is obtained by means of the FE analysis in an iterative fashion, using a global nonlinear solver. The load increment is controlled by time. Once the problem has being solved at time $t$, the solution for the next time increment requires the polycrystal model to provide a tangent stiffness (Jacobian) matrix $\boldsymbol{C}^{\mathrm{tg}} = \partial\Delta\boldsymbol{\sigma}/\partial\Delta\boldsymbol{\varepsilon}$ for each material point, in order for the FE scheme to compute an initial guess for the nodal displacements at $t + \Delta t$. The strain increments obtained from that prediction at each material point, $\Delta\boldsymbol{\varepsilon}^{\mathrm{FE}}$, together with the stress $\boldsymbol{\sigma}^{\mathrm{t}}$ and the set of internal state variables corresponding to the previous increment, are used inside UMAT to calculate a new guess for the stress and the Jacobian at $t + \Delta t$. When convergence in stress equilibrium is achieved by the global nonlinear scheme, the new values (at $t + \Delta t$) of the stresses, the internal variables, and the Jacobian matrix are accepted for every node, and the calculation advances to the next increment. For a given $\Delta\boldsymbol{\varepsilon}^{\mathrm{FE}}$, the VPSC-based UMAT is based on the minimization procedure described in [6] and is summarized here.

The elastic constitutive relation for the stress in the material point at $t + \Delta t$:

$$\boldsymbol{\sigma}^{\mathrm{t}+\Delta\mathrm{t}} = \boldsymbol{\sigma}^{\mathrm{t}} + \boldsymbol{C} : \Delta\boldsymbol{\varepsilon}_{\mathrm{el}} = \boldsymbol{\sigma}^{\mathrm{t}} + \boldsymbol{C} : \left(\Delta\boldsymbol{\varepsilon} - \Delta\boldsymbol{\varepsilon}_{\mathrm{vp}}\right) \tag{10}$$

where $\boldsymbol{C}$ is the elastic stiffness of the polycrystal. In this context, the natural choice for $\boldsymbol{C}$ is to use the elastic self-consistent (ELSC) estimate. Note that an ELSC calculation for the

determination of $\boldsymbol{C}$ is implemented in the VPSC code, at the beginning of each deformation increment. Hence, the textural changes are also accounted for in determining the elastic modulus of the polycrystalline material element.

Using Eq. (10) and the viscoplastic constitutive relation, we obtain:

$$\Delta\boldsymbol{\varepsilon} = \boldsymbol{C}^{-1} : \Delta\sigma + \Delta t\, \dot{\boldsymbol{\varepsilon}}_{vp}^{(px)}\left(\boldsymbol{\sigma}^{t} + \Delta\boldsymbol{\sigma}\right) \tag{11}$$

For a given trial strain increment $\Delta\boldsymbol{\varepsilon}^{\mathrm{FE}}$, we define the residual $\mathbf{X}(\Delta\boldsymbol{\sigma})$ at each material point as a nonlinear function of the stress increment $\Delta\boldsymbol{\sigma} = \boldsymbol{\sigma}^{\mathrm{t+\Delta t}} - \boldsymbol{\sigma}^{\mathrm{t}}$:

$$\mathbf{X}(\Delta\boldsymbol{\sigma}) = \Delta\boldsymbol{\varepsilon} - \Delta\boldsymbol{\varepsilon}^{FE} = \boldsymbol{C}^{-1} : \Delta\boldsymbol{\sigma} + \Delta t\, \dot{\boldsymbol{\varepsilon}}_{vp}^{(px)}\left(\boldsymbol{\sigma}^{t} + \Delta\boldsymbol{\sigma}\right) - \Delta\boldsymbol{\varepsilon}^{FE} \tag{12}$$

The condition $\mathbf{X}(\Delta\boldsymbol{\sigma}) = 0$ (i.e. $\Delta\boldsymbol{\varepsilon} = \Delta\boldsymbol{\varepsilon}^{\mathrm{FE}}$), is enforced using a Newton-Raphson (NR) scheme to solve the nonlinear system of equations. The corresponding Jacobian $\boldsymbol{J}_{\mathrm{NR}}$ is given by:

$$\begin{aligned} &\frac{\partial \mathbf{X}(\Delta\boldsymbol{\sigma})}{\partial(\Delta\boldsymbol{\sigma})} = \boldsymbol{J}_{NR}(\Delta\boldsymbol{\sigma}) = \boldsymbol{C}^{tg} = \\ &\quad = \boldsymbol{C}^{-1} + \Delta t\, \frac{\partial \dot{\boldsymbol{\varepsilon}}_{vp}^{(px)}}{\partial(\Delta\boldsymbol{\sigma})}\left(\boldsymbol{\sigma}^{t} + \Delta\boldsymbol{\sigma}\,;\, \beta_i^{t}\right) = \boldsymbol{C}^{-1} + \Delta t\, \boldsymbol{M}^{(px)}\left(\boldsymbol{\sigma}^{t} + \Delta\boldsymbol{\sigma}\right) \end{aligned} \tag{13}$$

Hence, given a guess $\Delta\boldsymbol{\sigma}^{\mathrm{k-1}}$ for the stress increment, the new guess is obtained as:

$$\Delta\boldsymbol{\sigma}^{\mathrm{k}} = \Delta\boldsymbol{\sigma}^{\mathrm{k-1}} - \boldsymbol{J}_{\mathrm{NR}}^{-1}\left(\Delta\boldsymbol{\sigma}^{\mathrm{k-1}}\right) : \mathbf{X}\left(\Delta\boldsymbol{\sigma}^{\mathrm{k-1}}\right) \tag{14}$$

This approach provides a closed expression for the FE Jacobian as a function of the viscoplastic tangent moduli (calculated as part of the VPSC algorithm), the elastic stiffness of the aggregate, and the FE time increment. The use of this expression greatly reduces the overall computational cost, because the polycrystal's stress and the elasto-viscoplastic tangent stiffness tensor are obtained from the same calculation loop. Moreover, the FE Jacobian allows for the quadratic convergence of the macroscopic nonlinear equations.

### Validation of the VPSC-based UMAT for Uranium

We first compare the results of the ABAQUS-VPSC implementation, against stand-alone (SA) VPSC calculations, for cases involving homogenous polycrystalline properties and simple boundary conditions, i.e. the type of configuration the stand-alone VPSC model can handle. For this purpose, we used straight rolled polycrystalline uranium in its annealed condition. The initial texture shown in Fig. 1 was represented by 1000 weighted orientations. The VPSC constitutive parameters for uranium are taken from a previous study on the same material [5].

Simple tension, simple compression, and simple share tests were simulated with the VPSC-based UMAT and compared with SA-VPSC for an applied deformation of 0.2. We considered the simple FE model of a single linear element C3D8 (8 nodes, and 8 integration points) with displacements imposed along the 2-direction for compression and tension and stress-free boundary conditions on the lateral faces. The simple shear of the same element was simulated for

an applied deformation gradient $\mathbf{F} = \mathbf{I} + \gamma\, \mathbf{e}_2 \otimes \mathbf{e}_3$, with $\gamma = 0.2$. This analysis was performed in order to check the correct treatment of rotations under finite-deformation kinematics. The predicted stress-strain curves and pole figures predicted by the two models are in excellent agreement (see Figs. 2-4).

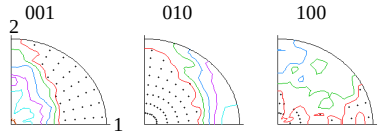


Figure 1: Pole figures showing the initial texture in the as-annealed uranium.

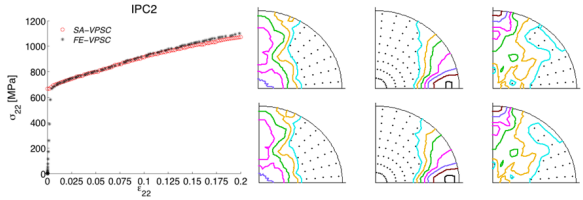


Figure 2: Predictions of the FE-VPSC UMAT described here compared with the corresponding predictions of SA-VPSC for compression in 2 direction of uranium: stress-strain curves and pole figures at strain of 0.2 (SA-VPSC top row and FE-VPSC bottom row).

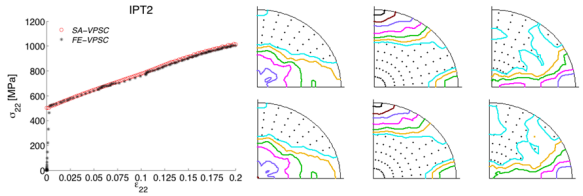


Figure 3: Predictions of the FE-VPSC UMAT described here compared with the corresponding predictions of SA-VPSC for tension in 2 direction of uranium: stress-strain curves and pole figures at strain of 0.2 (SA-VPSC top row and FE-VPSC bottom row).

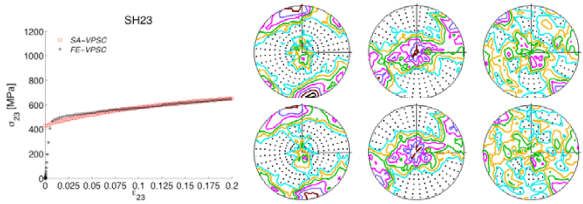


Figure 4 Predictions of the FE-VPSC UMAT described here compared with the corresponding predictions of SA-VPSC for simple shear in 23 direction of uranium: stress-strain curves and pole figures at strain of 0.2 (SA-VPSC top row and FE-VPSC bottom row).

Finally, simple compression experiments were performed on cylinders cut from a textured (see Fig. 1) uranium (straight rolled) sheet in two different directions, the rolling direction (1) and the through-thickness direction (3). These tests were used to further validate the implemented FE-VPSC UMAT and illustrate the strong effect of texture-induced anisotropy on the mechanical response of uranium. The geometrical changes of the samples are shown in Fig. 5. The FE model consisted of approximately 1000 C3D8 elements with the same 1000 grains at each integration point (see Fig. 1). Our results indicate the presence of a significant anisotropy in the material flow. The accuracy of our simulation results relative to the geometrical changes observed experimentally, demonstrate that the VPSC-based UMAT implementation adequately captures the complex deformation behavior (texture-induced anisotropy) observed in uranium.

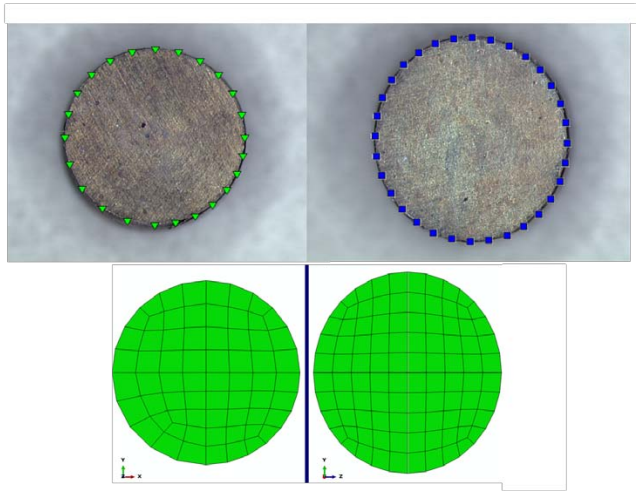

Figure 5: Comparison of predictions using the VPSC-based UMAT and experimentally measured cross-sections of cylinders compressed up to strain of 0.2 in the direction 3 (on the left) and in the direction 1 (on the right). The external nodal coordinates of the deformed FEM model are superimposed on the experimentally deformed samples of uranium.

**Acknowledgement**

This work was supported in part by the US Department of Energy under contract number DE-AC52-06NA25396 .

**References**

1. R. A. Lebensohn and C. N. Tomé, 'A self-consistent anisotropic approach for the simulation of plastic deformation and texture development of polycrystals: Application to zirconium alloys', *Acta Metallurgica et Materialia* 41 (1993) 2611-24.
2. R. A. Lebensohn, C. N. Tome and P. Ponte Castaneda, 'Self-consistent modelling of the mechanical behaviour of viscoplastic polycrystals incorporating intragranular field fluctuations', *Philosophical Magazine* 87 (2007) 4287-322.
3. M. Knezevic, H. F. Al-Harbi and S. R. Kalidindi, 'Crystal plasticity simulations using discrete Fourier transforms', *Acta Materialia* 57 (2009) 1777-84.
4. S. R. Kalidindi, C. A. Bronkhorst and L. Anand, 'Crystallographic Texture Evolution in Bulk Deformation Processing of Fcc Metals', *Journal of the Mechanics and Physics of Solids* 40 (1992) 537-69.
5. M. Knezevic, L. Capolungo, Carlos N. Tome, R. A. Lebensohn, D. J. Alexander, B. Mihaila and R. J. McCabe, 'Anisotropic stress-strain response and microstructure evolution of textured α-uranium', *Acta Materialia* in press (2011).
6. J. Segurado, R. A. Lebensohn, J. Llorca and C. N. Tomé, 'Multiscale modeling of plasticity based on embedding the viscoplastic self-consistent formulation in implicit finite elements', *International Journal of Plasticity* 28 (2012) 124-40.
7. R. J. McCabe, L. Capolungo, P. E. Marshall, C. M. Cady and C. N. Tomé, 'Deformation of wrought uranium: Experiments and modeling', *Acta Materialia* 58 (2010) 5447-59.
8. I. J. Beyerlein and C. N. Tomé, 'A dislocation-based constitutive law for pure Zr including temperature effects', *International Journal of Plasticity* 24 (2008) 867-95.
9. G. Proust, C. N. Tomé and G. C. Kaschner, 'Modeling texture, twinning and hardening evolution during deformation of hexagonal materials', *Acta Materialia* 55 (2007) 2137-48.